European flounder foraging movements in an estuarine nursery seascape inferred from otolith microchemistry and stable isotopes

Nils Teichert, Anne Lizé, Hélène Tabouret, Jean-Marc Roussel, Gilles Bareille, Thomas Trancart, Anthony Acou, Laure-Sarah Virag, Christophe Pécheyran, Alexandre Carpentier, et al.

HAL Id: hal-03843206
https://hal.inrae.fr/hal-03843206

Submitted on 22 Mar 2023

1   European flounder foraging movements in an estuarine nursery seascape

2   inferred from otolith microchemistry and stable isotopes

3   Short Title: Fish foraging movements in nursery seascape

4   Nils Teichert [1,2], Anne Lizé [1,2,3], Hélène Tabouret [4], Jean-Marc Roussel [5,6], Gilles Bareille [4],

5   Thomas Trancart [1,2], Anthony Acou [6,7], Laure-Sarah Virag [2], Christophe Pécheyran[4], Alexandre

6   Carpentier[8] & Eric Feunteun [1,2]

7   [1] UMR 7208 BOREA (MNHN, CNRS, IRD, SU, UCN, UA), Laboratoire de Biologie des Organismes et

8   Ecosystèmes Aquatiques, Paris, France.

9   [2] MNHN, Station Marine de Dinard, CRESCO, Dinard, France.

10   [3] School of Life Sciences, University of Liverpool, Liverpool, UK.

11   [4] Université de Pau et des Pays de l'Adour, E2S UPPA, CNRS, IPREM, Pau, France.

12   [5] DECOD (Ecosystem Dynamics and Sustainability), INRAE, IFREMER, Institut Agro, Rennes, France

13   [6] MIAME (Management of Diadromous Fish in their Environment), OFB, INRAE, Institut Agro, Université

14   de Pau, Rennes, France.

15   [7] Centre d'expertise et de données PatriNat (OFB – CNRS – MNHN), Station marine de Dinard, CRESCO,

16   Dinard, France.

17   [8] Université de Rennes 1, UMR 7208 BOREA (MNHN, CNRS, IRD, SU, UCN, UA), Campus de Beaulieu,

18   35000 Rennes, France.

19

20   Corresponding author: nils.teichert@mnhn.fr

21   Number of words in the abstract: 134 words

22   Number of words in the main text: 6056 words

23   Number of references: 71 references

24   Number of tables: 2 tables

25   Number of figures: 8 figures

1

26   **Abstract**

27   Despite the importance of estuarine nurseries in the regulation of many fish stocks, temporal and

28   spatial movements and habitat use patterns of juvenile fish remain poorly understood. Overall,

29   combining several movement metrics allowed us to characterize dispersal patterns of juvenile flounder,

30   *Platichthys flesus,* along an estuarine seascape. Specifically, we investigated otolith microchemistry

31   signatures (Sr:Ca and Ba:Ca ratios) and stable isotope ratios (δ^{13}C and δ^{15}N) in muscles of these juveniles,

32   during three consecutive years to assess inter-annual fluctuations in their home range and isotopic

33   niches. The morphological condition and lipid content of individuals were lower in years of high as

34   compared to low dispersal along the estuarine gradient. We discuss these results in relation to the

35   ecosystem productivity and intra- and inter-specific competition level, which in turn affects movements

36   and foraging behaviors of juvenile flounders.

37   **Keywords**: *Platichthys flesus*; Nursery; Otolith chemistry; Isotopes; Feeding strategy; Estuary;
38   Dispersion; Home range

39

40

2

1. Introduction

Estuaries are complex ecosystems at the interface between marine and freshwater environments, associated with numerous ecological functions and ecosystem services (Barbier et al., 2011). In particular, estuaries provide diverse ecological niches to estuarine, freshwater, marine and diadromous fish (Potter et al., 2015), which benefit from the estuarine productivity during early stages of their life cycle (Sheaves et al., 2015). Evaluating the nursery value of estuarine habitats requires understanding resource dynamic and availability, connectivity patterns and ontogenetic migration of fish (Nagelkerken et al., 2015; Sheaves et al., 2015). Indeed, the quality of a nursery depends particularly on its ability to provide refuges against predators, and trophic resources (Beck et al., 2001). Changes in these conditions can therefore impact individual growth and morphological condition with ultimate consequences on survival and stock recruitment (Vasconcelos et al., 2009). Fluctuations of the estuarine productivity and/or competition pressures can thus lead to inter-annual variations of the nursery value, but also in habitat used and movement patterns of individuals (e.g. Mendes et al., 2014; Schloesser and Fabrizio, 2019). When resources are limited and/or patchily distributed, individuals are expected to increase foraging movements to find their food, leading to additional metabolic costs (Bowler and Benton, 2005). Conversely, when resources are abundant and evenly distributed, juveniles are expected to limit costly movements and promote sedentary lifestyle while increasing their physiological condition.

Although nursery habitats are known to regulate many fish stocks (Beck et al., 2001), movement and dynamics of habitat use by early life stages of fish remain poorly understood in estuaries (Reis-Santos et al., 2015). Several tagging approaches are available for assessing connectivity patterns and home range of large fish (e.g. Le Pichon *et al.*, 2014). However, these methods are generally technically and/or ethically unsuitable for small vertebrates (Gillanders, 2009). Conversely, biological tracers of fish can deliver relevant information on connectivity patterns and home range of small-bodied fish, providing there is enough environmental heterogeneity (Elsdon et al., 2008; Secor et al., 1995). Biological tracers, such as the chemical composition of fish otoliths, or stable isotope ratios in soft

3

66   tissues and internal organs, have already demonstrated their usefulness to investigate fish movements

67   among adjacent or segregated habitats within estuaries (e.g. Green *et al.*, 2012; Reis-Santos *et al.*, 2015;

68   Mohan & Walther, 2018).

69   Carbon (^{13}C) and nitrogen (^{15}N) stable isotope ratios can be quantified in various fish tissues,

70   including mucus, blood, fin, scale, liver or muscle, and these values reflect the spatial variation in food

71   sources and position of the studied species in the food web (Hobson, 1999). During trophic transfer, the

72   isotopic compositions of the consumer tissues compare to its prey change with variations in diet

73   sources, tissue-specific turnover (i.e. time taken for a tissue to regenerate) and fractionation (i.e. how

74   tissues fractionate the different isotopes and change the isotopic ratios) (Caut et al., 2009). Therefore,

75   the time required to reach a new isotopic equilibrium when the fish feed on a new food source is

76   dependent on the tissue specific metabolic activity with, for example, higher turnover rates for the liver

77   or blood than for muscle tissues (Buchheister and Latour, 2010). Accordingly, resident fish are expected

78   to exhibit stable isotopic ratios aligned with local food webs, whereas immigrant fish may display mixed

79   signatures or larger isotopic niches (Cunjak et al., 2005; Fry et al., 2003; Reis-Santos et al., 2015). A

80   gradual decrease in carbon isotope ratios (δ^{13}C) is expected along the salinity gradient from sea to

81   freshwater through estuarine habitats (Herzka, 2005; Hobson, 1999; Peterson and Fry, 1987; Reis-

82   Santos et al., 2015). δ^{13}C ratio primarily reflects variations in algal or detrital C sources at the bottom of

83   the food chains (e.g. Kostecki et al., 2012, 2010), while the nitrogen isotope ratio (δ^{15}N) increases with

84   trophic levels from preys to predators through ^{15}N accumulation (Peterson and Fry, 1987). Spatial

85   changes in δ^{15}N ratio are generally induced by anthropogenic activities (Herzka, 2005; Mohan and

86   Walther, 2018). In estuarine nurseries, investigating shifts in stable C and N isotopic composition can be

87   useful to estimate the proportion of migrant and resident fish, as well as the home range of their early

88   life stages (Charles et al., 2004; Green et al., 2012; Herzka, 2005; Mohan and Walther, 2018; Reis-Santos

89   et al., 2015). However, stable C and N isotopic values of immigrant will dilute within few days or weeks

90   depending on tissue investigated, meaning that evidences of migration will fade relatively quickly after

91   settlement and feeding in their new habitat, the nursery (Cunjak et al., 2005).

4

92   While stable isotope ratios provide an overview of organism movement and feeding behavior, the

93   otolith chronological properties allow reconstructing patterns of habitat used and migration histories

94   over long period (Secor et al., 1995). When a fish moves between habitats with distinct chemical

95   signatures, some chemical elements are incorporated in the aragonitic matrix of its otoliths according

96   to their different concentrations in the chemically distinct habitats (Daverat et al., 2005; Hüssy et al.,

97   2020). Hence, the profile of chemical elements along an otolith transect records the fish movements

98   between these habitats (Campana, 1999). Although a large panel of chemical elements can be tracked,

99   not all provide information on the surrounding habitats, and some of them are more influenced by the

100   fish physiology than by its environment (e.g. Mg, Limburg et al., 2018). Strontium:Calcium (Sr:Ca) and

101   Barium:Calcium (Ba:Ca) elemental ratios are known to reflect changes in ambient water, while being

102   little influenced by the fish physiology (Daverat et al., 2005; Hüssy et al., 2020). In estuarine waters, the

103   Sr:Ca ratio commonly declines with the salinity gradient, while the Ba:Ca ratio increases in response to

104   the growing freshwater input (Elsdon and Gillanders, 2006, 2005; Tabouret et al., 2010). These opposite

105   dual patterns have thus been exploited to highlight fish migrations, and their movements at small-scale

106   along the salinity gradient (Daverat et al., 2012; Laugier et al., 2015; Reis-Santos et al., 2015; Teichert et

107   al., 2022; Williams et al., 2018). Using laser ablation-inductively coupled to a plasma mass spectrometer

108   (LA-ICP-MS), the elementary signatures of otoliths can be quantified on very thin structures of three to

109   ten µm wide, which respectively represents one day to a few weeks of a fish life (e.g. Selleslagh et al.,

110   2016). Comparisons between the otolith and estuarine seascape elemental compositions provide a

111   quantitative assessment of movement extent and home range during early life stages of a fish.

112   Among the fish species using estuaries as nursery areas, the flatfish European flounder,

113   *Platichthys flesus* (Linnaeus, 1758), is widespread throughout the European coasts, from the White,

114   Mediterranean to the Black seas. Flounders exhibit a facultative catadromous life cycle. Although

115   spawning typically occurs in marine coastal waters, some individuals spawn in brackish or freshwater

116   areas (Daverat et al., 2012). After hatching, larvae use selective tidal transport to reach estuarine

117   nursery areas (Bos, 1999), where they generally settle in shallow upper reaches subjected to freshwater

5

118   influence (Bos and Thiel, 2006; Mendes et al., 2020). Although some individuals remain in freshwater

119   for few years, older juveniles tend to move toward the middle or lower sections of the estuary (Amorim

120   et al., 2018). Juvenile flounders are generalist feeders, but the young-of-the-year (i.e. 0+) tend to feed

121   on fewer preys, essentially amphipods of the genus *Corophium* (e.g. Mendes et al., 2020). By contrast,

122   the diet composition of larger individuals is more diversified, including small polychaetes and

123   oligochaetes (Mendes et al., 2020, 2014; Summers, 1980). Large juveniles exhibit restricted home

124   ranges and high site fidelity as demonstrated by mark–recapture surveys (Dando, 2011) and telemetry

125   studies (Le Pichon et al., 2014; Wirjoatmodjo and Pitcher, 1984). However, the movement patterns of

126   early settled flounders across estuarine seascape are far less known, mainly because of their small size

127   (total length <90 mm). Given their specific diet, 0+ flounders are expected to strongly depend on prey

128   availability and repartition, foraging on potentially large areas to find them.

129   In this study, we used biological tracers to investigate movement patterns of flounder juveniles in

130   the Sélune estuary (Lower-Normandy, Western France) during three consecutive years. Specifically,

131   both otolith microchemistry signatures (Sr:Ca and Ba:Ca ratios) and stable isotope ratios (δ^{13}C and δ^{15}N)

132   in muscle tissues were used to reconstruct home range and isotopic niches of juveniles. We

133   hypothesized that inter-annual fluctuations in patterns of mobility and foraging behaviour will reflect in

134   the morphological condition and lipid content of fish juveniles.

135   ## 2.   Materials and methods

136   ### *2.1. Study area and fish sampling*

137   *2.1.1.   Study area*

138   The Sélune River flows over 91 km from the source to the English Channel in the Mont Saint-Michel

139   Bay, Lower-Normandy, France (Fig. 1). The catchment is 1 106 km² and median river discharge is 5.56

140     $m^3.s^{-1}$ at the river mouth. Since 1919, the upper part of the river network was disconnected (827 km²)

141   by two large hydroelectric power dams (La-Roche-qui-Boit, H=16m, and Vezins, H=36 m). However,

6

142 environmental authorities and local operators decided to remove these two dams to restore the

143 ecological continuity in compliance with the EU Water Framework Directive. Vezins dam (located 23 km

144 upstream the estuary) was teared down in 2020, and removal of La-Roche-Qui-Boit dam (18 km

145 upstream the estuary) will be achieved in 2023. Even if flounders are limited to the estuarine area and

146 dams did not disturb their distribution on the river catchment, the input of nutriments and terrigenous

147 organic matter into the estuary was likely affected during dismantling operations. The macro-tidal Mont

148 Saint-Michel bay has the second highest tidal range in Europe (average: 10-11m and up to 16m) and its

149 large intertidal zone covers 220 km^2 (Laffaille et al., 2001). During ebb tides in the Sélune estuary, the

150 water supply is primarily ensured by river discharges, while the tidal influence during flood tides is

151 perceptible up to the confluence with the Oir River (Fig.1). Accordingly, large salinity variations occur

152 along the estuary, with highest fluctuations recorded in middle reaches, as observed in comparable

153 macro-tidal estuaries (Robins et al., 2014). Salinity at the confluence between the Sée and Sélune rivers

154 (Fig. 1) ranged from 2 to 34 ‰ during low and high tides respectively (Kostecki et al., 2012; unpublished

155 data, Nils Teichert). In such estuaries, the influence of marine tidal flux dominates in the lower reaches

156 leading to higher salinity range at high tide, but decreases toward upstream as inputs of freshwater

157 increase. Therefore, the distance to the sea appeared to be a more relevant descriptor than punctual

158 salinity measures to assess the marine influence along the estuary continuum. Here, we defined the

159 distance to the sea (d_s, in km) as the distance between each estuarine position and the accepted limit

160 of the transitional waters, following the main channel of the Sélune River (Fig. 1).

161   Daily records of river discharges were provided by the DREAL Basse-Normandie for the Ducey

162 hydrological station (ref. I9241010), which is located on the Sélune River bank, just upstream of the tidal

163 influence. Sampling was done during low hydrological conditions in late summer for three consecutive

164 years; the mean (± sd) river discharge ($m^3.s^{-1}$) during the month prior the samplings differed significantly

165 between the three years (F = 45.54, p < 0.001), ranging from 1.85 $m^3.s^{-1}$ (± 0.75) in 2019 to 2.45 $m^3.s^{-1}$

166 (± 0.61) in 2020 and 3.31 $m^3.s^{-1}$ (± 0.44) in 2021. However, these freshwater inputs remained far below

7

167   the median river discharge (5.56 $m^3.s^{-1}$), which suggests little estuarine salinity variation during the

168   studied periods.

169   *2.1.2.   Fish sampling*

170   In the first year (2019), juvenile flounders were collected in autumn at six sites along the Sélune

171   estuarine continuum (Fig. 1, Table 1) to investigate isotopic and elemental signatures (see thereafter

172   for method details). At site 1, 13 juvenile flounders were collected using a beam trawl (1.5 m large, 16

173   mm mesh size) during high tide in September 2019. At site 2 and 3, 31 and 5 flounders were collected

174   using a pushnet in September and November 2019 respectively, while 3, 8 and 4 flounders were

175   respectively caught at sites 4, 5 and 6 by electrofishing in September 2019. Note that the upstream

176   repartition of flounders was limited by two small weirs (approximatively 1 m high) located upstream of

177   sites 5 and 6 (Fig.1). Based on this first year of study, highest abundance of juvenile flounders was

178   recorded at site 3, and this site was chosen to investigate movement patterns over in 2020 and 2021.

179   Juveniles were collected using a pushnet (n = 31 and 34 in September 2020 and 2021, respectively). All

180   collected fish were anesthetized with a Benzocaine solution (15 mg.L^{-1}) before being euthanized with a

181   Benzocaine overdosed solution (200 mg.L^{-1}), and then frozen (-20°C) until dissections at the laboratory.

182   Juvenile flounders were measured (total length (TL) in mm) and weighed (total weight (TW) in g) to

183   determine their morphological conditions using a length-independent relative condition index (Jakob et

184   al., 1996). To this end, we fitted a linear regression model between the log-transformed body mass and

185   standard length (log(TW) = - 12.15 + 3.14 x log(TL), R^2 = 0.966, p < 0.001), where model residuals were

186   then used as an index of body condition, with positive and negative residuals representing increased

187   and decreased body condition respectively.

188   **2.2. Analysis of otolith microchemistry**

189   *2.2.1.   Otolith preparation and elemental quantification*

190   Flounder sagittal otoliths were extracted and embedded in epoxy resin (Araldite 2020, Huntsman

191   Corporation), then grounded along the transversal plane, and polished until the primordium was

8

192 reached. The otolith elemental composition (Sr and Ba) was quantified using femtosecond laser ablation

193 (LA, IR 1030 nm; Alfamet-Novalase, France) coupled with an inductively plasma mass spectrometer (ICP-

194 MS, DRCII; Perkin Elmer, Shelton). Ablations were performed with a raster scanning strategy along the

195 longest growth axis of each otolith with a laser beam of 15 μm of diameter, at a frequency of 20 Hz,

196 moving forward at 5 μm.s^{-1}. Although each laser ablation was conducted from the primordium to the

197 external edge of otolith, our analysis focused on the latest 150 μm to study the last month of the juvenile

198 life. The resulting elementary profile thus consisted of successive records taken every 5 μm,

199 approximately representing one day of the juvenile flounder life (Amara et al., 2009), as also reported

200 in the Sélune estuary (unpublished data, Nils Teichert). The external calibration was done by using the

201 international reference materials NIST614, NIST612 and NIST610 (National Institute of Standards and

202 Technology, USA). Calcium, an internal standard, is used to account for variations in the amount of

203 ablation material and laser energy in ablation efficiency. Therefore, elementary compositions were

204 standardized in elementary mass ratios, Sr:Ca and Ba:Ca. Analytical precision was measured using the

205 otolith certified reference materials: fish NIES22 (National Institute for Environmental Studies, Japan;

206 Yoshinaga, Nakama, Morita, & Edmonds, 2000) and FEBS-1 (National Research Council Canada, Canada).

207 *2.2.2. Spatio-temporal changes in marginal otolith signatures*

208 We investigated spatial changes in elemental composition along the estuarine gradient using the

209 otolith marginal signatures of Sr:Ca and Ba:Ca ratios. This approach assumes that the signature at the

210 otolith external edge, which corresponds to the last period of a fish life, indicates the chemical signature

211 of their habitat just before being caught. The signatures of the two last elemental records from the

212 otolith edge (i.e. 10 μm, around 2 days) were compared between the six sampling sites using a

213 permutation-based approach (permanova), with the Manhattan distance to account for dissimilarity

214 between the scales of elemental ratios. For each elemental ratio, relationships between marginal

215 signatures and the distance to the sea were then investigated using non-parametric Spearman

216 correlation tests. Finally, the temporal consistency of otolith signatures was verified by comparing the

217 marginal signatures of flounders caught at site 3 for the three sampling years, using a permanova.

9

218   *2.2.3.   Inferring longitudinal positions from otolith signatures*

219   Longitudinal positions (i.e. distance to the sea) of flounders were estimated by fitting a Generalized

220   Additive Model (GAM) adjusted with the otolith marginal signatures corresponding to the last two days

221   of the fish before being caught (i.e. 10 µm). GAM model allows to estimate non-linear response curves

222   (Wood, 2000). In the GAM model, the distance to the sea was used as response variable and the

223   marginal elemental records as predictors, which were associated with cubic smoothing splines. The

224   interaction between Sr:Ca and Ba:Ca ratios was considered in the model because preliminary

225   examination indicated that its inclusion slightly improved the Akaike's information criterion (delta AIC :

226   13.2 between models without and with interaction). All the marginal records were included in the model

227   adjustment process, except for some flounders caught at site 3. At this site, a random sample of 30

228   flounders was selected for fitting the model, whereas the other fish were used to evaluate the model

229   performances on independent data. The significance and performance of the model were then tested

230   using a deviance reduction test (F-test) and the adjusted r-squared (R_{adj}) respectively. In addition, the

231   positioning error (km) was calculated as the absolute distance separating the predicted position from

232   the location of sampling site.

233   *2.2.4.   Inter-annual movements inferred from otolith signatures*

234   Elemental records from the last 150 µm of the otolith edge were used in the GAM model to predict

235   successive positions of juvenile flounders during the month prior to the sampling. This distance

236   threshold (i.e. 150 µm) corresponds roughly to a mean daily growth rate of 5 $\mu m.d^{-1}$, which is consistent

237   with previous observations in other estuaries of similar characteristics in the English Channel (Amara et

238   al., 2009). The predicted positions (i.e. distance to the sea) were used to calculate synthetic metrics

239   reflecting how settled flounders occupied and moved along the estuarine seascape during the month

240   preceding their capture (Table 2). While four metrics reflect how each individual used the longitudinal

241   gradient (i.e. longitudinal position, individual niche extent, daily niche extent and daily niche used), the

242   metric 'population niche extent' encompasses the estuarine gradient used by all caught fish of the year

243   (i.e. annual cohort). Individual metrics were calculated for each fish caught at site 3 and inter-annual

10

244   differences (i.e. 2019, 2020 and 2021) were then investigated using an ANOVA, followed by pairwise

245   comparisons with post-hoc Tukey HSD tests. For each sampling year, the population niche extent was

246   estimated using bootstrap resampling with 1000 replicates. The niche extent for each year was

247   considered statistically different from one another if the 95% confidence intervals did not overlap.

248   ### *2.3. Analysis of stable isotopes in fish muscles*

249   #### *2.3.1. Quantification of stable isotopes*

250   For each collected fish, one muscle tissue sample was dissected to estimate its trophic position and

251   origin of food sources based on its nitrogen and carbon isotopic signatures (Table 2, Hobson, 1999).

252   Isotopic signatures were expressed in the delta unit notation as deviation from international standards

253   of PeeDee Belemnite for $\delta^{13}C$ and atmospheric N_2 for $\delta^{15}N$, following the formula: $\delta X =$

254   ((Rsample/Rstandard)-1) x 1000), where X is ^{13}C or ^{15}N and R is the ratio (^{15}N:^{14}N or ^{13}C:^{12}C) in the sample

255   and in the standard. For each muscle sample, nitrogen and carbon total quantities, and the isotopic

256   ratios were measured by continuous flow isotope mass spectrometry (CF-IRMS) using a Thermo

257   Scientific Delta V Advantage mass spectrometer coupled to a Thermo Scientific Flash 2000 elemental

258   analyzer. Analytical precision (standard deviation) was < 0.15‰ of reference material. We considered

259   that correction of $\delta^{13}C$ values for lipid-rich tissues was not necessary because the ratio of carbon relative

260   to nitrogen (C:N ratio) in muscle samples were almost all < 3.3, and exceptionally of 3.6 (Post et al.

261   2007). Moreover, the C:N ratio was used as a proxy of lipid content stored in fish muscle

262   (McConnaughey and McRoy, 1979; Mohan and Walther, 2018; Post et al., 2007). For each fish, the

263   percentage of lipid content was estimated based on the C:N ratio following the linear approximation

264   proposed by Post et al. (2007) for aquatic animals (% lipid = -20.54 + 7.24 x C:N).

265   #### *2.3.2. Inter-annual variations of isotopic niches*

266   Using fish collected at six sites, we first examined variations of isotopic ratios ($\delta^{13}C$ and $\delta^{15}N$) along

267   the longitudinal estuarine gradient by investigating their linear relationships between the distance to

268   the sea to sampling sites, and the longitudinal positions inferred from otolith signatures. We then

269   compared the annual isotopic signatures of fish caught at site 3 using an ANOVA, followed by post-hoc

270   Tukey HSD tests, to investigate inter-annual changes in resource origin and trophic level (Table 2).

271   Finally, we estimated the isotopic niche sizes for each year at site 3, from a 2D kernel density estimation

272   at 95% confidence level using δ^{13}C and δ^{15}N values (Eckrich et al., 2020). We generated 1000 bootstrap

273   replicates of isotopic niche size to determine significant differences between years, based on non-

274   overlapping 95% confidence intervals.

275   All statistical analyses were performed in the R environment v. 4.0.5 (R Core Team, 2018) using the

276   'stats' package for standard analysis, such as linear regressions, ANOVA and Tukey HSD post-hoc tests.

277   The GAM models were adjusted using the 'mgcv' package (Wood, 2011). Kernel density estimation of

278   isotopic niches were performed using the 'rKIN' package (Eckrich et al., 2020) and bootstrap replicates

279   were generated using the 'boot' library (Canty and Ripley, 2017).

280   3. Results

281   Overall, juvenile flounders used to assess spatial variability in isotopic and elemental signatures

282   (sites 1, 2, 4, 5 and 6) were significantly larger (TL between 32 and 205 mm, Table 1) than those caught

283   at site 3 ($F = 57.21$, $p < 0.001$). In this latter nursery site, the total length (TL) of 0+ juveniles ranged from

284   27 to 75 mm (mean = 41.5 mm) and differed significantly between the three sampling years, with larger

285   sizes in 2021 ($F = 14.18$, $p < 0.001$) (Fig. 2a). The juvenile condition was significantly higher in 2020 than

286   in other years for the morphological condition index ($F = 6.51$, $p = 0.002$; Fig. 2b) and the lipid content

287   in muscles inferred from C:N ratio ($F = 6.65$, $p = 0.002$; Fig. 2c).

288   *3.1. Spatio-temporal changes in marginal otolith signatures*

289   Bivariate otolith marginal signatures varied significantly between sampling sites ($R^2 = 0.54$, $F = 60.7$,

290     $p < 0.001$; Fig. 3). Following non-linear trends, the Ba:Ca elemental ratio increased (rho = 0.56, $p <$

291   0.001), while the Sr:Ca decreased significantly with the distance to the sea (rho = -0.71, $p < 0.001$).

12

292 Signatures at site 3 remained similar between years (R^2 = 0.02, F = 2.11, p = 0.095), which emphasized

293 the temporal consistency of otolith signatures. By extension, we postulate that this is also the case

294 across the estuarine gradient.

295 *3.2. Inferring movements from otolith microchemistry*

296 The GAM model adjusted from otolith marginal signatures explained 83.4% of deviance of the

297 distance to the sea (R^2_{adj} = 0.81, F = 27.51, p < 0.001). The predicted distance increased with increasing

298 Ba:Ca ratio and decreasing Sr:Ca ratio, according to nonlinear relationships (Fig. 4). The mean (± SD)

299 positioning error was 2.46 (± 2.46) km for all records used for model adjustment, while it was 2.12 ±

300 (1.93) km and 1.87 (± 1.81) km respectively for the adjustment and validation of subsamples of fish

301 caught at site 3.

302 Focusing on juvenile flounders caught at site 3, individual movement metrics revealed inter-annual

303 differences during the last month of the fish life (Fig. 5). In 2021, juvenile flounders used upper estuarine

304 habitats as revealed by the significant change in median longitudinal positions (F = 5.99, p = 0.003). In

305 2019, the individual niche extent was two time larger than for other years (F = 27.7, p < 0.001), indicating

306 that flounders used a larger range of estuarine habitats during lower hydrological conditions. Also, the

307 daily niche extent decreased significantly from 2019 to 2021 (F = 20.9, p < 0.001), which suggests a

308 lower propensity to disperse as freshwater flows increase. In comparison to the other years, juvenile

309 flounders caught in 2020 traveled daily on a significantly larger part of their spatial niche (F = 20.9, p <

310 0.001). At the population level, the niche extent displayed an opposite pattern where juvenile flounders

311 caught in 2020 explored a narrower estuarine gradient than in other years, which stressed the low

312 propensity of fish to disperse in 2020 (Fig. 6).

313 *3.3. Stable isotope signatures and trophic niches*

314 δ^{13}C values in fish muscles were significantly related to the distance to the sea of the sampling sites

315 (R^2 = 0.506, F = 129.08, p < 0.001). Interestingly, the relationship was even stronger using the

316 longitudinal estuarine positions inferred from otolith signatures (R^2 = 0.725, F = 340.17, p < 0.001),

13

317   suggesting that some individuals have recently immigrated in the sampling site (Fig. 7). By contrast, $\delta^{15}N$

318   values did not vary with longitudinal estuarine positions of juvenile flounders (R^2 = 0.00, F = 0.024, p =

319   0.874).

320   For juvenile flounders caught at site 3, $\delta^{13}C$ signatures were slightly lower in 2021 in comparison to

321   the other years (F = 17.70, p = 0.002), which appears congruent with upper positions previously

322   highlighted by otolith signatures (Fig. 8). The trophic level, reflected by $\delta^{15}N$ signatures, was higher in

323   2019 (F = 11.47, p < 0.001), suggesting that preys consumed by juvenile flounders or their nitrogen

324   signatures were different from the two other years. At the population scale, the isotopic niche size

325   estimated for juvenile flounders caught in 2020 was very thin, indicating that individuals fed on a

326   restricted range of prey items (Fig. 8). By contrast, isotopic niches of juvenile flounders caught in 2019

327   and 2021 were much larger than in 2020, suggesting greater heterogeneity of food resources used by

328   individuals.

329   ## 4. Discussion

330   ### 4.1. Biological tracers in estuarine environment

331   Estuarine seascapes provide a suitable context to investigate animal movements based on

332   environmental tracers because of the gradual changes in local conditions (Williams et al., 2018),

333   including water chemistry (Walther and Nims, 2015). As reported in previous studies, Sr:Ca and Ba:Ca

334   elemental ratios recorded in fish otoliths displayed opposite relationships with salinity, so that their

335   simultaneous use provides a useful indication on fish position along the salinity gradient (e.g. Elsdon &

336   Gillanders, 2005; Tabouret et al., 2010; Daverat et al., 2011, 2012; Reis-Santos et al., 2015; Williams et

337   al., 2018; Nelson & Powers 2020). Here, we used the distance to the sea as a proxy of the estuarine

338   continuum, mainly because sharp changes in local salinity induced by tides appeared poorly suitable to

339   interpret otolith signatures. Despite the high laser beam resolution, the 5 μm elemental records yielded

340   a buffered daily signature, which was insufficient to capture salinity variations over tidal cycle, but rather

14

341 reflected a spatial pattern shaped by the extent of marine intrusion along the estuary. This longitudinal

342 discrimination was thus particularly relevant to reconstruct juvenile fish movements across the

343 estuarine nursery (Mohan and Walther, 2018; Williams et al., 2018).

344   In the same way, $\delta^{13}C$ signature variations in flounder juvenile muscles clearly reflected the

345 estuarine gradient, with highest values at the vicinity of the sea. Analogous results have been reported

346 in other estuaries (e.g. Reis-Santos et al., 2015). These results allow to discriminate the origin of preys

347 consumed by fish (Green et al., 2012; Mendes et al., 2020), as well as the relative contribution of marine

348 and freshwater organic matters at the bottom of the food web (França et al., 2011; Kostecki et al., 2012,

349 2010; Selleslagh et al., 2015). Accordingly, isotopic signatures can be used to infer foraging extents and

350 fish movements, as geochemical gradients are reflected in tissues of locally foraging organisms (Winter

351 et al., 2021). Additionally, fish assignments can depict their locations several days or weeks prior to the

352 capture because of the isotopic turnover rate in fish muscles. Here, we assumed that the observed

353 signatures reflected resources accumulated over one month before the fish sampling, which is in

354 accordance with the turnover rates generally reported for fish juveniles (Herzka, 2005). This assumption

355 was also supported by the congruence between $\delta^{13}C$ signatures and longitudinal positions inferred from

356 otolith signatures, which correctly relocated juvenile flounders that recently immigrated in the sampling

357 sites.

358   Both otolith elemental and muscle isotopic signatures appeared as decisive tools for investigating

359 fish spatial patterns in estuaries. However, exogenous factors such as river flow inputs, tidal cycles or

360 wave energy can induce spatial variability in local environmental conditions, and limit or even impair

361 the interpretation of movements inferred by natural tracers (e.g. Gillanders, 2005; Elsdon & Gillanders,

362 2006). For a stationary estuarine location, the intensification of river flow is expected to decrease the

363 Sr:Ca ratio, while increasing the Ba:Ca ratio, in response to the extra freshwater input (Walther and

364 Nims, 2015; Williams et al., 2018). The inverse trend should be expected when the marine intrusion is

365 enhanced, such as when the river flow is low, or during spring tides. In the present study, we

15

366 demonstrated that otolith marginal signatures of juvenile flounders caught in the median part of the

367 estuary (site 3) remained stable over the three sampling years, while the river discharges were different.

368 This result confirms the steadiness of microchemical signatures over the range of river flow considered

369 in this study (during the low flow summer period). Unfortunately, the whole estuarine gradient was not

370 sampled over the three years, so we had to assume stability of spatial patterns across the estuary.

371 *4.2. Home range and movements across the seascape nursery*

372 We took advantage of the estuarine gradient to reconstruct small scale movements of juvenile

373 flounders using a GAM model, which accounted for the non-linearity relation between otolith elemental

374 ratios and salinity (Nelson and Powers, 2020). The simultaneous use of Sr:Ca and Ba:Ca substantially

375 increased the model performance, leading to a mean positioning error of about 2 km, less than 7% of

376 the estuarine length. Coherently with the stable C isotopes turnover rates in fish muscles, juvenile

377 flounders' movements were reconstructed over the last month of their life, by focusing on the

378 elemental records from the last 150 μm of the otolith edge. We thus assumed a constant otolith growth

379 rate between individual (i.e. 5 $\mu m.d^{-1}$) because daily age estimates based on microstructures were

380 difficult to obtain using otoliths prepared for elemental analysis.

381 Overall, movement metrics demonstrated the important site fidelity of early-settled juvenile

382 flounders in the Sélune estuary. The individual niche extent over one month was restricted to about 6

383 km during the drought hydrological year and about 3 km when the river flow was higher. This result is

384 in accordance with studies highlighting that juvenile flounders forage on inundated mudflats at high

385 tide, but remain in the main tidal channel supplied by the river flow during low tides (Summers, 1980;

386 Wirjoatmodjo and Pitcher, 1984). Juvenile flounders are thus subjected to important physicochemical

387 variations induced by tides, while juveniles of other marine species, such as sea bass for instance, reach

388 the intertidal areas at high tide, and then move back to marine subtidal areas at low tide (Laffaille et al.,

389 2001; Teichert et al., 2018). Even in the Sélune macro-tidal estuary, the resident behaviour of juvenile

390 flounders resulted in small daily movements along the estuarine gradient (on average between 400 and

16

391   800 m), which emphasizes that they can find suitable foraging, sheltering and resting conditions in a

392   reduced spatial extend. Similar results have been reported for late-stage juvenile flounders (2+, 3+) and

393   mature flounders that moved respectively about 870 m (Le Pichon et al., 2014), and 270 m on average

394   during one tidal cycle (Wirjoatmodjo and Pitcher, 1984).

395   Both isotopic and elemental signatures also highlighted inter-annual differences in the distribution

396   of juvenile flounders, which tended to use upper estuarine habitats in 2021. It is probable that annual

397   modifications in hydro-morphological conditions and in the spatial availability of prey contribute to the

398   changes in their longitudinal positions. The prey availability has been reported as an essential driver of

399   0+ flounder movements and their distribution in the nursery habitat (Bos, 1999; Florin and Lavados,

400   2010; Mendes et al., 2020). Moreover, the Sélune estuary is part of the Mont-Saint Michel bay, and is

401   therefore subjected to important sediment movements that recurrently modify the structure of tidal

402   channels and the distribution of estuarine habitats (Levoy et al., 2017). Interestingly, the individual niche

403   extent was larger in 2019, which suggests that individuals explored a longer range of the estuarine

404   gradient maybe in response to lower resources availability during this year. In this case, the spatial

405   distribution of food resources and competition for its accessibility must be the main drivers of individual

406   mobility and home range of juveniles across the nursery seascape (Bolnick et al., 2003).

407   *4.3. Inter-annual changes in foraging movements*

408   Overall, our results revealed that the morphological condition and lipid storage of juvenile

409   flounders, estimated from C:N ratio, were higher in 2020 than in 2019 and 2021. Our hypothesis to

410   explain this is that inter-annual fluctuations lead to variations in ecosystem productivity and competition

411   level, which in turn affects patterns of mobility and foraging behaviors of fish juveniles. Indeed, when

412   resources are abundant and evenly distributed, individuals are expected to disperse regularly over small

413   spatial niches because food accessibility is not a limiting factor (MacArthur and Pianka, 1966). In this

414   case, the reduced energy cost of small-scale displacements and food abundance should increase

415   individual condition, and their energetic reserves. Conversely, if resources are scarce or unevenly

17

416   distributed, individuals should display a more marked exploration behaviour to find their food and

417   potentially face competition (Lesser et al., 2020; Svanbäck and Bolnick, 2007). In such a case, resources

418   used by the population is expected to be more diversified and individual spatial niches larger and less

419   depleted in terms of resources on a daily basis. Consequently, food limitation and energy expenditure

420   caused by movements and competition are expected to decrease the individual reserves and

421   morphological condition.

422   Here, isotopic niches and population niche extents displayed convergent annual patterns,

423   highlighting that juvenile flounders caught in 2020 were in good condition and dispersed little, feeding

424   on a restricted range of prey items. These fish efficiently used their individual niche extent as evaluated

425   by the daily niche used ratio, which suggests that individuals can daily cross a large part of their home

426   range, in search of suitable habitats and sufficient resources to grow and accumulate energy reserves.

427   Contrastingly, the large spatial and isotopic niche sizes reported for the 2019 and 2021 populations

428   could reflect an increase of intra-specific competition, where individuals had to adopt different foraging

429   strategies and use distinct estuarine locations (Bolnick et al., 2003). Interestingly, processes involved in

430   niche sizes delineation were likely different between years. In 2019, the large population niche extent

431   was associated with an increase in the extent of individual niches, whereas they remained narrow in

432   2021 but scattered along the estuarine gradient. This result confirms that changes in population niche

433   size can be decoupled from changes in the individual niches within the population (Bolnick et al., 2010).

434   During these periods, where juvenile flounders were in low condition, the daily use of individual spatial

435   niches was less efficient than in 2020, suggesting that travel for daily activities was likely more expensive,

436   either because of the involved distances and/or linked to hydrological constraints. Although our study

437   does not clearly highlight the mechanism shaping the spatial and trophic niches of juvenile flounders,

438   our results emphasize the strong inter-annual variability of their trophic movements. This variability is

439   probably related to changes in resource availability and biotic interactions within the nursery. Future

440   studies should thus focus on linking individual and population dispersal patterns with environmental

18

441   constraints, such as prey availability, conspecific abundance, competition, and/or the presence of

442   predators.

5. Credit authorship contribution statement

444   **Nils Teichert**: Conceptualization, Project administration, Funding acquisition, Data curation,

445   Methodology, Formal analysis, Writing - original draft. **Anne Lizé, Hélène Tabouret, Gilles Bareille,**

446   **Anthony Acou, Thomas Trancart**: Methodology, Data curation, Writing - review & editing. **Jean-Marc**

447   **Roussel**: Writing - review & editing. **Laure-sarah Virag**: Methodology, Data curation. **Alexandre**

448   **Carpentier, Eric Feunteun**: Conceptualization, Funding acquisition, Methodology, Supervision, Writing -

449   review & editing.

6. Declaration of Competing Interest

451   The authors declare that they have no known competing financial interests or personal relationships

452   that could have appeared to influence the work reported in this article.

7. Data Availability

454   Data that support the findings of this study are available from the corresponding author upon

455   reasonable request.

8. Acknowledgements

19

461   during the field survey. This study was approved by the Cuvier Ethic Committee (project n°68-106), the

462   local representative of the French national ethic committee for animal in research.

9. References

464   Amara, R., Selleslagh, J., Billon, G., Minier, C., 2009. Growth and condition of 0-group European flounder,
465   *Platichthys flesus* as indicator of estuarine habitat quality. Hydrobiologia 627, 87–98.

466   Amorim, E., Ramos, S., Elliott, M., Bordalo, A.A., 2018. Dynamic habitat use of an estuarine nursery
467   seascape: Ontogenetic shifts in habitat suitability of the European flounder (*Platichthys flesus*). J.
468   Exp. Mar. Bio. Ecol. 506, 49–60.

469   Barbier, E.B., Hacker, S.D., Kennedy, C., Koch, E.W., Stier, A.C., Silliman, B.R., 2011. The value of estuarine
470   and coastal ecosystem services. Ecol. Monogr. 81, 169–193.

471   Beck, M.W., Heck, K.L., Able, K.W., Childers, D.L., Eggleston, D.B., Gillanders, B.M., Halpern, B., Hays,
472   C.G., Hoshino, K., Minello, T.J., 2001. The identification, conservation, and management of
473   estuarine and marine nurseries for fish and invertebrates: a better understanding of the habitats
474   that serve as nurseries for marine species and the factors that create site-specific variability in
475   nurse. Bioscience 51, 633–641.

476   Bolnick, D.I., Ingram, T., Stutz, W.E., Snowberg, L.K., Lau, O.L., Paull, J.S., 2010. Ecological release from
477   interspecific competition leads to decoupled changes in population and individual niche width.
478   Proc. R. Soc. B Biol. Sci. 277, 1789–1797.

479   Bolnick, D.I., Svanbäck, R., Fordyce, J.A., Yang, L.H., Davis, J.M., Hulsey, C.D., Forister, M.L., 2003. The
480   ecology of individuals: incidence and implications of individual specialization. Am. Nat. 161, 1–28.

481   Bos, A.R., 1999. Aspects of the life history of the European flounder (*Pleuronectes flesus* L. 1758) in the
482   tidal river Elbe. Dissertation. de.

483   Bos, A.R., Thiel, R., 2006. Influence of salinity on the migration of postlarval and juvenile flounder
484   *Pleuronectes flesus* L. in a gradient experiment. J. Fish Biol. 68, 1411–1420.

485   Bowler, D.E., Benton, T.G., 2005. Causes and consequences of animal dispersal strategies: relating
486   individual behaviour to spatial dynamics. Biol. Rev. 80, 205–225.

487   Buchheister, A., Latour, R.J., 2010. Turnover and fractionation of carbon and nitrogen stable isotopes in
488   tissues of a migratory coastal predator, summer flounder (*Paralichthys dentatus*). Can. J. Fish.
489   Aquat. Sci. 67, 445–461.

490 Campana, S.E., 1999. Chemistry and composition of fish otoliths: pathways, mechanisms and
491   applications. Mar. Ecol. Prog. Ser. 188, 263–297.

492 Canty, A., Ripley, B., 2017. boot: Bootstrap R (S-Plus) Functions. R package version 1.3-20. R Packag.
493   version 1.3-20.

494 Caut, S., Angulo, E., Courchamp, F., 2009. Variation in discrimination factors (Δ15N and Δ13C): The effect
495   of diet isotopic values and applications for diet reconstruction. J. Appl. Ecol. 46, 443–453.

496 Charles, K., Roussel, J.-M., Cunjak, R.A., 2004. Estimating the contribution of sympatric anadromous and
497   freshwater resident brown trout to juvenile production. Mar. Freshw. Res. 55, 185–191.

498 Cunjak, R.A., Roussel, J.-M., Gray, M.A., Dietrich, J.P., Cartwright, D.F., Munkittrick, K.R., Jardine, T.D.,
499   2005. Using stable isotope analysis with telemetry or mark-recapture data to identify fish
500   movement and foraging. Oecologia 144, 636–646.

501 Dando, P.R., 2011. Site fidelity, homing and spawning migrations of flounder *Platichthys flesus* in the
502   Tamar estuary, South West England. Mar. Ecol. Prog. Ser. 430, 183–196.

503 Daverat, F., Martin, J., Fablet, R., Pécheyran, C., 2011. Colonisation tactics of three temperate
504   catadromous species, eel *Anguilla anguilla*, mullet *Liza ramada* and flounder *Plathychtys flesus*,
505   revealed by Bayesian multielemental otolith microchemistry approach. Ecol. Freshw. Fish 20, 42–
506   51.

507 Daverat, F., Morais, P., Dias, E., Babaluk, J., Martin, J., Eon, M., Fablet, R., Pécheyran, C., Antunes, C.,
508   2012. Plasticity of European flounder life history patterns discloses alternatives to catadromy. Mar.
509   Ecol. Prog. Ser. 465, 267–280.

510 Daverat, F., Tomas, J., Lahaye, M., Palmer, M., Elie, P., 2005. Tracking continental habitat shifts of eels
511   using otolith Sr/Ca ratios: validation and application to the coastal, estuarine and riverine eels of
512   the Gironde–Garonne–Dordogne watershed. Mar. Freshw. Res. 56, 619–627.

513 Eckrich, C.A., Albeke, S.E., Flaherty, E.A., Bowyer, R.T., Ben-David, M., 2020. rKIN: Kernel-based method
514   for estimating isotopic niche size and overlap. J. Anim. Ecol. 89, 757–771.

515 Elsdon, T.S., Gillanders, B.M., 2006. Temporal variability in strontium, calcium, barium, and manganese
516   in estuaries: implications for reconstructing environmental histories of fish from chemicals in
517   calcified structures. Estuar. Coast. Shelf Sci. 66, 147–156.

518 Elsdon, T.S., Gillanders, B.M., 2005. Alternative life-history patterns of estuarine fish: barium in otoliths
519   elucidates freshwater residency. Can. J. Fish. Aquat. Sci. 62, 1143–1152.

21

520 Elsdon, T.S., Wells, B.K., Campana, S.E., Gillanders, B.M., Jones, C.M., Limburg, K.E., Secor, D.H.,
521   Thorrold, S.R., Walther, B.D., 2008. Otolith chemistry to describe movements and life-history
522   parameters of fishes: hypotheses, assumptions, limitations and inferences. Oceanogr. Mar. Biol.
523   an Annu. Rev. 46, 297–330.

524 Florin, A.-B., Lavados, G., 2010. Feeding habits of juvenile flatfish in relation to habitat characteristics in
525   the Baltic Sea. Estuar. Coast. Shelf Sci. 86, 607–612.

526 França, S., Vasconcelos, R.P., Tanner, S., Máguas, C., Costa, M.J., Cabral, H.N., 2011. Assessing food web
527   dynamics and relative importance of organic matter sources for fish species in two Portuguese
528   estuaries: a stable isotope approach. Mar. Environ. Res. 72, 204–215.

529 Fry, B., Baltz, D.M., Benfield, M.C., Fleeger, J.W., Gace, A., Haas, H.L., Quiñones-Rivera, Z.J., 2003. Stable
530   isotope indicators of movement and residency for brown shrimp (*Farfantepenaeus aztecus*) in
531   coastal Louisiana marshscapes. Estuaries 26, 82–97.

532 Gillanders, B.M., 2009. Tools for studying biological marine ecosystem interactions—natural and
533   artificial tags, in: Ecological Connectivity among Tropical Coastal Ecosystems. Springer, pp. 457–
534   492.

535 Gillanders, B.M., 2005. Using elemental chemistry of fish otoliths to determine connectivity between
536   estuarine and coastal habitats. Estuar. Coast. Shelf Sci. 64, 47–57.

537 Green, B.C., Smith, D.J., Grey, J., Underwood, G.J.C., 2012. High site fidelity and low site connectivity in
538   temperate salt marsh fish populations: A stable isotope approach. Oecologia 168, 245–255.

539 Herzka, S.Z., 2005. Assessing connectivity of estuarine fishes based on stable isotope ratio analysis.
540   Estuar. Coast. Shelf Sci. 64, 58–69.

541 Hobson, K.A., 1999. Tracing origins and migration of wildlife using stable isotopes: a review. Oecologia
542   120, 314–326.

543 Hüssy, K., Limburg, K.E., de Pontual, H., Thomas, O.R.B., Cook, P.K., Heimbrand, Y., Blass, M., Sturrock,
544   A.M., 2020. Trace element patterns in otoliths: the role of biomineralization. Rev. Fish. Sci. Aquac.
545   29(4), 445-477.

546 Jakob, E.M., Marshall, S.D., Uetz, G.W., 1996. Estimating fitness: a comparison of body condition indices.
547   Oikos 77, 61–67.

548 Kostecki, C., Le Loc'h, F., Roussel, J.-M., Desroy, N., Huteau, D., Riera, P., Le Bris, H., Le Pape, O., 2010.
549   Dynamics of an estuarine nursery ground: the spatio-temporal relationship between the river flow

550 and the food web of the juvenile common sole (*Solea solea*, L.) as revealed by stable isotopes

551 analysis. J. Sea Res. 64, 54–60.

552 Kostecki, C., Roussel, J.-M., Desroy, N., Roussel, G., Lanshere, J., Le Bris, H., Le Pape, O., 2012. Trophic

553 ecology of juvenile flatfish in a coastal nursery ground: contributions of intertidal primary

554 production and freshwater particulate organic matter. Mar. Ecol. Prog. Ser. 449, 221–232.

555 Laffaille, P., Lefeuvre, J.-C., Schricke, M.-T., Feunteun, E., 2001. Feeding ecology of o-group sea bass,

556 *Dicentrarchus labrax*, in salt marshes of Mont Saint Michel Bay (France). Estuaries 24, 116–125.

557 Laugier, F., Feunteun, E., Pecheyran, C., Carpentier, A., 2015. Life history of the Small Sandeel,

558 *Ammodytes tobianus*, inferred from otolith microchemistry. A methodological approach. Estuar.

559 Coast. Shelf Sci. 165, 237–246.

560 Le Pichon, C., Trancart, T., Lambert, P., Daverat, F., Rochard, E., 2014. Summer habitat use and

561 movements of late juvenile European flounder (*Platichthys flesus*) in tidal freshwaters: results from

562 an acoustic telemetry study. J. Exp. Mar. Bio. Ecol. 461, 441–448.

563 Lesser, J.S., James, W.R., Stallings, C.D., Wilson, R.M., Nelson, J.A., 2020. Trophic niche size and overlap

564 decreases with increasing ecosystem productivity. Oikos 129, 1303–1313.

565 Levoy, F., Anthony, E.J., Dronkers, J., Monfort, O., Izabel, G., Larsonneur, C., 2017. Influence of the 18.6-

566 year lunar nodal tidal cycle on tidal flats: Mont-Saint-Michel Bay, France. Mar. Geol. 387, 108–113.

567 Limburg, K.E., Wuenschel, M.J., Hüssy, K., Heimbrand, Y., Samson, M., 2018. Making the otolith

568 magnesium chemical calendar-clock tick: plausible mechanism and empirical evidence. Rev. Fish.

569 Sci. Aquac. 26, 479–493.

570 MacArthur, R.H., Pianka, E.R., 1966. On optimal use of a patchy environment. Am. Nat. 100, 603–609.

571 McConnaughey, T., McRoy, C.P., 1979. Food-web structure and the fractionation of carbon isotopes in

572 the Bering Sea. Mar. Biol. 53, 257–262.

573 Mendes, C., Ramos, S., Bordalo, A.A., 2014. Feeding ecology of juvenile flounder *Platichthys flesus* in an

574 estuarine nursery habitat: Influence of prey–predator interactions. J. Exp. Mar. Bio. Ecol. 461, 458–

575 468.

576 Mendes, C., Ramos, S., Elliott, M., Bordalo, A.A., 2020. Feeding strategies and body condition of juvenile

577 European flounder *Platichthys flesus* in a nursery habitat. J. Mar. Biol. Assoc. UK. 100, 795–806.

578 Mohan, J.A., Walther, B.D., 2018. Integrating multiple natural tags to link migration patterns and

579 resource partitioning across a subtropical estuarine gradient. Estuaries and coasts 41, 1806–1820.

23

580   Nagelkerken, I., Sheaves, M., Baker, R., Connolly, R.M., 2015. The seascape nursery: a novel spatial
581   approach to identify and manage nurseries for coastal marine fauna. Fish Fish. 16, 362–371.

582   Nelson, T.R., Powers, S.P., 2020. Elemental concentrations of water and Otoliths as salinity proxies in a
583   northern Gulf of Mexico estuary. Estuaries and Coasts 43, 843–864.

584   Peterson, B.J., Fry, B., 1987. Stable isotopes in ecosystem studies. Annu. Rev. Ecol. Syst. 18, 293–320.

585   Post, D.M., Layman, C.A., Arrington, D.A., Takimoto, G., Quattrochi, J., Montana, C.G., 2007. Getting to
586   the fat of the matter: models, methods and assumptions for dealing with lipids in stable isotope
587   analyses. Oecologia 152, 179–189.

588   Potter, I.C., Tweedley, J.R., Elliott, M., Whitfield, A.K., 2015. The ways in which fish use estuaries: a
589   refinement and expansion of the guild approach. Fish Fish. 16, 230–239.

590   R Core Team, 2018. R: A language and environment for statistical computing. R Foundation for Statistical
591   Computing, Vienna, Austria. URL https//www.R-project.org/.

592   Reis-Santos, P., Tanner, S.E., França, S., Vasconcelos, R.P., Gillanders, B.M., Cabral, H.N., 2015.
593   Connectivity within estuaries: an otolith chemistry and muscle stable isotope approach. Ocean
594   Coast. Manag. 118, 51–59.

595   Robins, P.E., Lewis, M.J., Simpson, J.H., Malham, S.K., 2014. Future variability of solute transport in a
596   macrotidal estuary. Estuar. Coast. Shelf Sci. 151, 88–99.

597   Schloesser, R.W., Fabrizio, M.C., 2019. Nursery Habitat Quality Assessed by the Condition of Juvenile
598   Fishes: Not All Estuarine Areas Are Equal. Estuaries and Coasts 42, 548–566.

599   Secor, D.H., Henderson-Arzapalo, A., Piccoli, P.M., 1995. Can otolith microchemistry chart patterns of
600   migration and habitat utilization in anadromous fishes? J. Exp. Mar. Bio. Ecol. 192, 15–33.

601   Selleslagh, J., Blanchet, H., Bachelet, G., Lobry, J., 2015. Feeding Habitats, Connectivity and Origin of
602   Organic Matter Supporting Fish Populations in an Estuary with a Reduced Intertidal Area Assessed
603   by Stable Isotope Analysis. Estuaries and Coasts 38, 1431–1447.

604   Selleslagh, J., Echard, A., Pécheyran, C., Baudrimont, M., Lobry, J., Daverat, F., 2016. Can analysis of
605   *Platichthys flesus* otoliths provide relevant data on historical metal pollution in estuaries?
606   Experimental and in situ approaches. Sci. Total Environ. 557, 20–30.

607   Sheaves, M., Baker, R., Nagelkerken, I., Connolly, R.M., 2015. True Value of Estuarine and Coastal
608   Nurseries for Fish: Incorporating Complexity and Dynamics. Estuaries and Coasts 38, 401–414.

24

609   Summers, R.W., 1980. The diet and feeding behaviour of the flounder *Platichthys flesus* (L.) in the Ythan
610   estuary, Aberdeenshire, Scotland. Estuar. Coast. Mar. Sci. 11, 217–232.

611   Svanbäck, R., Bolnick, D.I., 2007. Intraspecific competition drives increased resource use diversity within
612   a natural population. Proc. R. Soc. B Biol. Sci. 274, 839–844.

613   Tabouret, H., Bareille, G., Claverie, F., Pécheyran, C., Prouzet, P., Donard, O.F.X., 2010. Simultaneous use
614   of strontium: calcium and barium: calcium ratios in otoliths as markers of habitat: application to
615   the European eel (*Anguilla anguilla*) in the Adour basin, South West France. Mar. Environ. Res. 70,
616   35–45.

617   Teichert, N., Carassou, L., Sahraoui, Y., Lobry, J., Lepage, M., 2018. Influence of intertidal seascape on
618   the functional structure of fish assemblages: Implications for habitat conservation in estuarine
619   ecosystems. Aquat. Conserv. Mar. Freshw. Ecosyst. 28(4), 798-809.

620   Teichert, N., Lizé, A., Tabouret, H., Gérard, C., Bareille, G., Acou, A., Carpentier, A., Trancart, T., Virag, L.-
621   S., Robin, E., Druet, M., Prod'Homme, J., Feunteun, E., 2022. A multi-approach study to reveal eel
622   life-history traits in an obstructed catchment before dam removal. Hydrobiologia 849(8), 1885-
623   1903.

624   Vasconcelos, R.P., Reis-Santos, P., Fonseca, V., Ruano, M., Tanner, S., Costa, M.J., Cabral, H.N., 2009.
625   Juvenile fish condition in estuarine nurseries along the Portuguese coast. Estuar. Coast. Shelf Sci.
626   82, 128–138.

627   Walther, B.D., Nims, M.K., 2015. Spatiotemporal variation of trace elements and stable isotopes in
628   subtropical estuaries: I. Freshwater endmembers and mixing curves. Estuaries and Coasts 38, 754–
629   768.

630   Williams, J., Jenkins, G.P., Hindell, J.S., Swearer, S.E., 2018. Fine-scale variability in elemental
631   composition of estuarine water and otoliths: Developing environmental markers for determining
632   larval fish dispersal histories within estuaries. Limnol. Oceanogr. 63, 262–277.

633   Winter, E.R., Hindes, A.M., Lane, S., Britton, J.R., 2021. Dual-isotope isoscapes for predicting the scale
634   of fish movements in lowland rivers. Ecosphere 12(4), e03456.

635   Wirjoatmodjo, S., Pitcher, T.J., 1984. Flounders follow the tides to feed: evidence from ultrasonic
636   tracking in an estuary. Estuar. Coast. Shelf Sci. 19, 231–241.

637   Wood, S.N., 2011. Fast stable restricted maximum likelihood and marginal likelihood estimation of
638   semiparametric generalized linear models. J. R. Stat. Soc. Ser. B 73, 3–36.

639   Wood, S.N., 2000. Modelling and smoothing parameter estimation with multiple quadratic penalties. J.

640   R. Stat. Soc. Ser. B 62, 413–428.

641

26

642   **Table 1:** Summary of the juvenile flounders*, Platichthys flesus*, collected in the six sampling sites of

643   the estuarine nursery of the Sélune River. The sampling date, number and fish size range (total length,

644   mm) are provided, as well as analyses in which they were involved. While all individuals were used to

645   investigate spatial change in otolith microchemistry and isotopic signatures along the estuarine

646   gradient, only fish from site 3 were used to describe the interannual variability of movement patterns

647   and trophic niches.

648

Site	Sampling date	Number	Size range (mm)	Analysis
1	28 Sept. 2019	13	35-91	spatial
2	12 Nov. 2019	5	32-53	spatial
3	16 Sept. 2019	31	27-65	spatial - temporal
3	17 Sept. 2020	31	30-50	spatial - temporal
3	17 Sept. 2021	34	33-75	spatial - temporal
4	9 Sept. 2019	3	43-113	spatial
5	9 Sept. 2019	8	48-187	spatial
6	23 Sept. 2019	4	142-205	spatial

649

650

651   **Table 2:** List of movement and isotopic metrics derived from otolith elemental and muscle isotopic
652   signatures of juvenile flounder, *Platichthys flesus*, in the estuarine nursery of the Sélune River.
653   Movement metrics derived from elemental records from the last 150 μm of the otolith edge reflect how
654   flounder occupied and moved along the estuarine seascape the month before their capture. The
655   biological level of each metric is specified such as Ind: individual, Pop: fish population sampled the same
656   year.

657

Metrics	Scale	Unit	Description
Otolith microchemistry			
Longitudinal position	Ind.	km	Median of distances to the sea predicted during the last month of fish, reflecting the average longitudinal position occupied by fish on the estuarine gradient.
Individual niche extent	Ind.	km	Absolute difference between quantiles 5% and 95% of predicted positions during the last month of the fish, estimating the longitudinal extent occupied by the fish along the estuarine gradient (i.e. distance between extreme positions).
Daily niche extent	Ind.	km	Median of distances between successive predicted positions during the last month of the fish, representing the average longitudinal distance traveled in a day, assuming an otolith daily growth rate of 5 μm.d^{-1}.
Daily niche used	Ind.	-	Ratio between the daily and individual niche extents, reflecting the amount of estuarine gradient traveled daily compared to the total extent used during the last month by the fish.
Population niche extent	Pop.	km	Absolute difference between upper and lower limits of the 95% kernel distribution density of longitudinal positions of fish population, representing the longitudinal extent occupied by the fish population along the estuarine gradient.
Muscle isotopy			
Resource origin	Ind.	‰	Carbon isotopic ratio (δ^{13}C), traducing variations in signatures of food sources consumed by the fish, which basically correspond to various contributions of terrigenous organic matter to the estuarine food web.
Trophic level	Ind.	‰	Nitrogen isotopic ratio (δ^{15}N), traducing the trophic level of fish through enrichment process from prey to predator or changes in δ^{15}N values at the basal level of the estuarine food web.
Isotopic niche size	Pop.	-	2D Kernel isotopic niche size estimated at the 95% confidence level, based on δ^{13}C and δ^{15}N values of the fish population. It reflects the amount of heterogeneity in food source and origin consumed by the population.

658

659

660

661
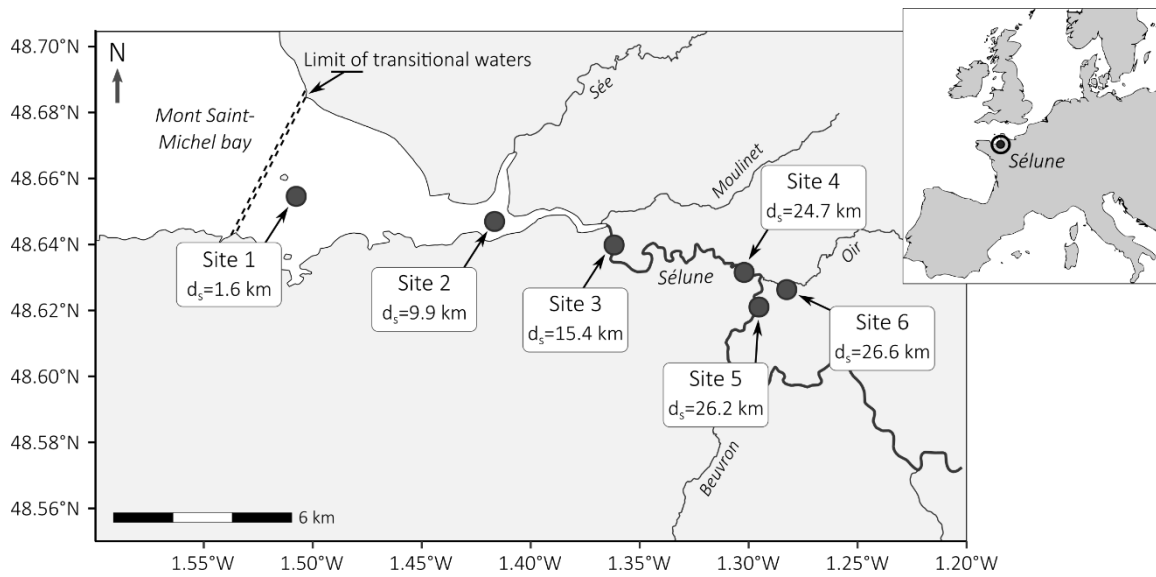
Figure 1: Location of the six sampling sites within the estuarine nursery of the Sélune River, Western Europe, France. The distance to the sea (d_s, km) is specified for each site, and corresponds to the distance from the limit of the transitional waters following the main river channel.
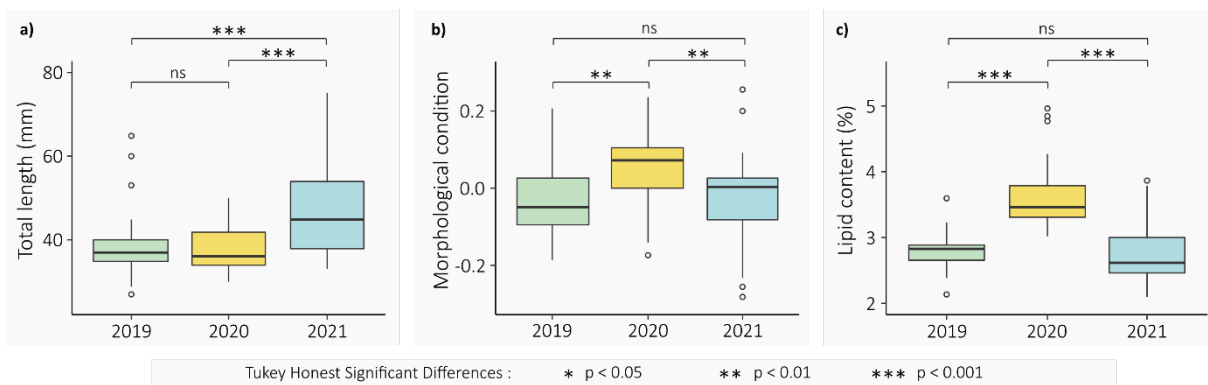
665

666

667

668

669

670

671

Figure 2: Biological traits of juvenile flounders, *Platichthys flesus*, caught at site 3 of the Sélune estuarine nursery in September 2019 (n = 31), 2020 (n = 31) and 2021 (n = 34). The boxplots show the a) total length (mm), b) morphological condition (no unit) and c) lipid content (%) whose estimation is based on the C:N ratio for each sampling year. Results of pairwise Tukey honest significant difference tests are provided.

677

678

29

679
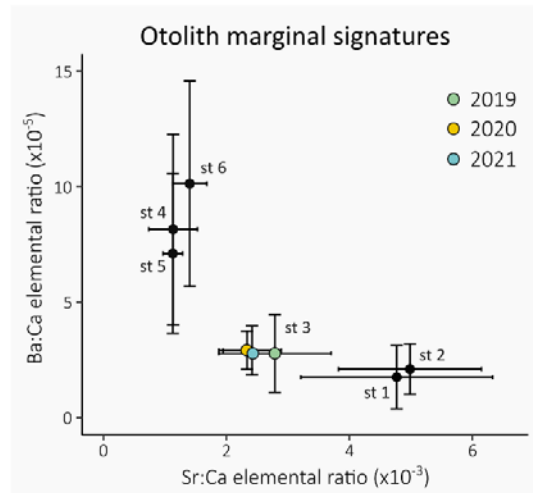
Figure 3: Spatio-temporal changes in otolith marginal signatures of juvenile flounders, *Platichthys flesus,* collected in the six sampling sites of the Sélune estuarine nursery. The bivariate plot displays the Sr:Ca and Ba:Ca mean elemental ratios recorded from the otolith edge (10 µm, around 2 days of life) according to sampling sites (st 1-6) and years for the site 3. Vertical bars represent standard deviations.

684

685

686
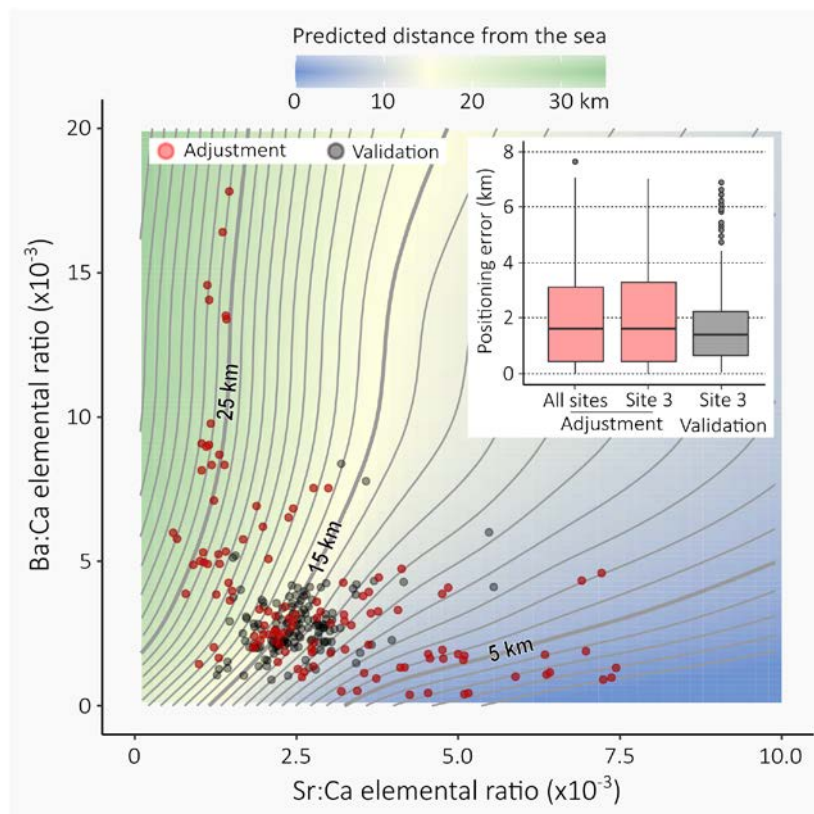
Figure 4: Isolines of distances to the sea predicted from the GAM model using Sr:Ca and Ba:Ca elemental ratios of juvenile flounder otoliths, caught et the six sampling sites of the Sélune estuarine nursery. Dots represent the marginal elemental records (10 µm, around 2 days of life) used to fit the model (red) and those used for validation purpose for site 3 (grey). The boxplot in the upper box details the positioning error (km) for the adjustment and validation subsamples.
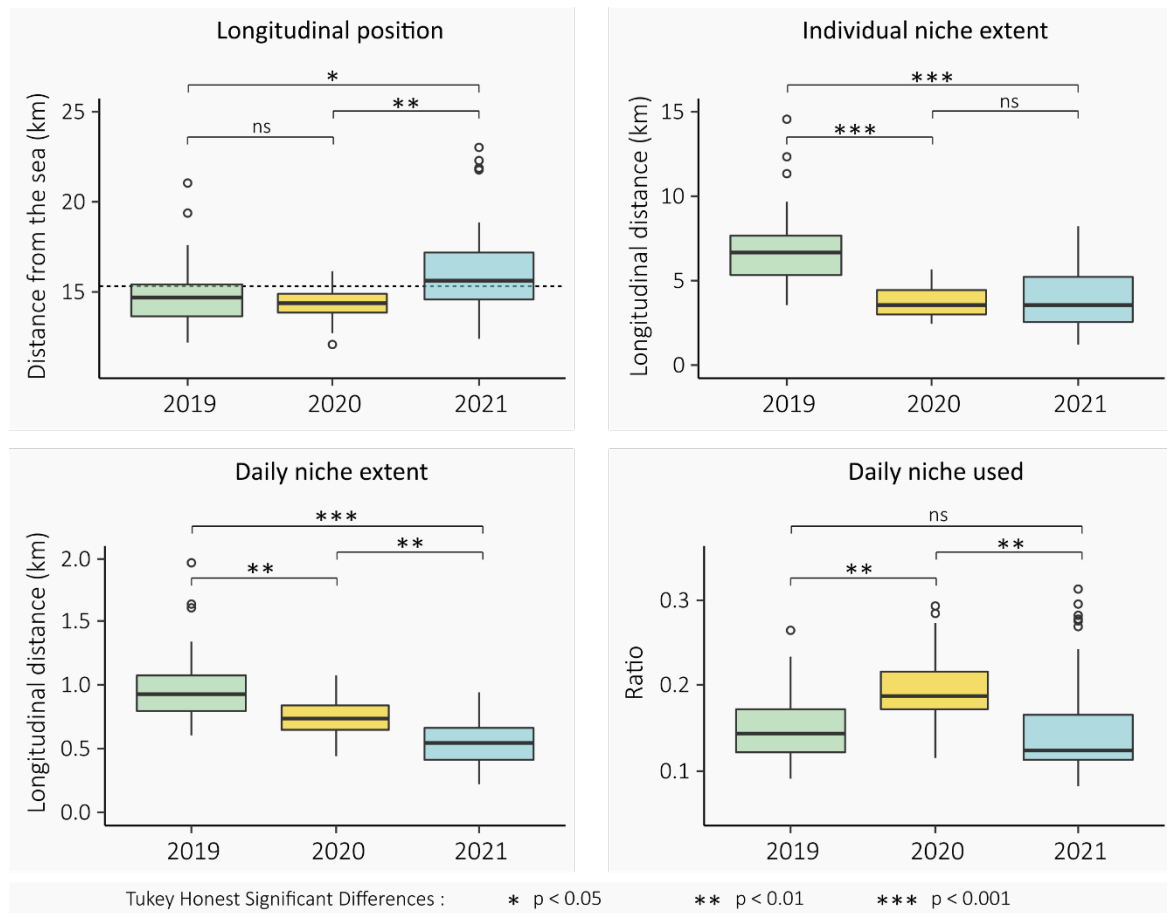
Figure 5: Inter-annual variations in longitudinal position, individual niche extent, daily niche extent and daily niche used by juvenile flounders, *Platichthys flesus,* caught at site 3 of SéBune estuarine nursery in 2019 (n = 31), 2020 (n = 31) and 2021 (n = 34). See Table 1 for a detailed description of each metric. The dashed line represents the longitudinal position of site 3. Results of pairwise Tukey honest significant differences tests are provided.
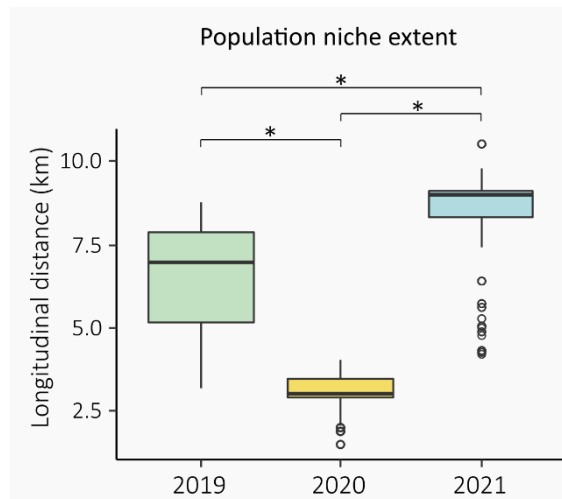
Figure 6: Population niche extent (km) of juvenile flounders caught at site 3 of the Sélune estuarine nursery in 2019 (n = 31), 2020 (n = 31) and 2021 (n = 34). See Table 1 for a detailed description of this metric. Boxplots show the niche extent generated from 1000 bootstrap replicates. Niche extends for each year were assumed to be statistically different from each other (*) if the 95% confidence intervals did not overlap.


2019   2020   2021
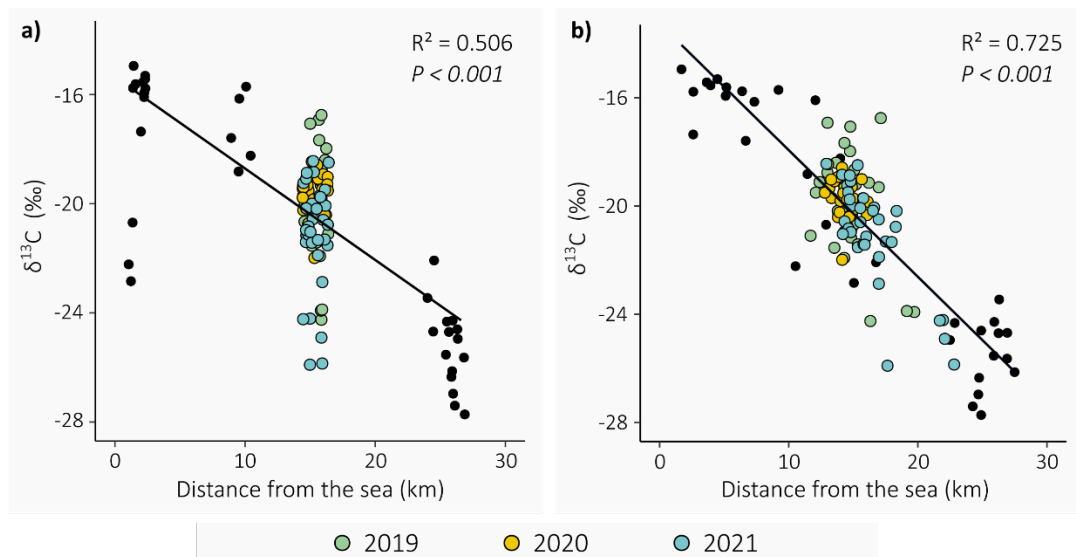
Figure 7: Linear relationship between the $\delta^{13}C$ signatures (‰) in muscle of juvenile flounders caught at the six sampling sites of the Sélune estuary and distance to the sea a) from its catching location and b) from its predicted location based on elemental composition of otoliths. Coloured dots represent the fish caught at site 3 for the three sampling years, while black ones gather fish caught at the other sites.
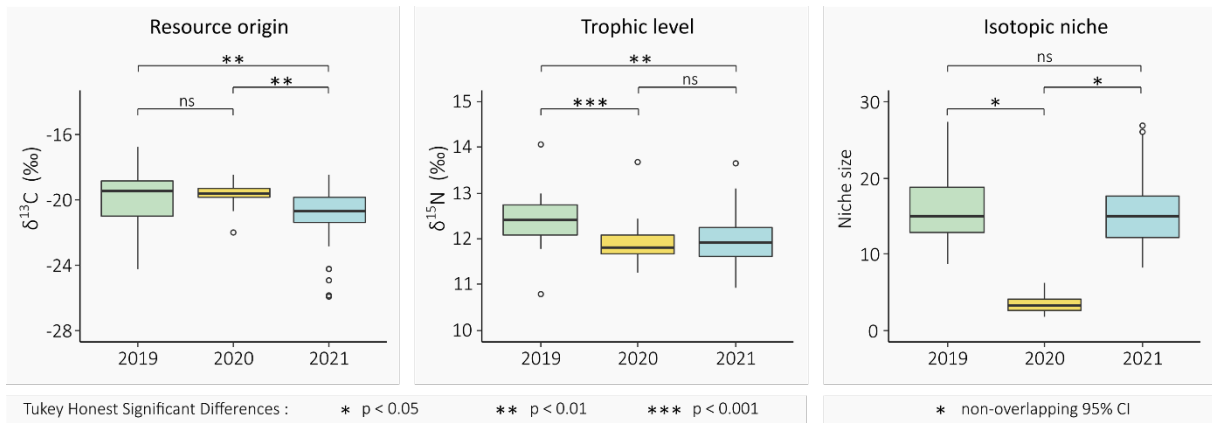
Figure 8: Inter-annual variations in resource origin (δ^{13}C, ‰), trophic level (δ^{15}N, ‰) and population isotopic niche size of juvenile flounders caught at site 3 of the Sélune estuarine nursery in 2019 (n = 31), 2020 (n = 31) and 2021 (n = 34). See Table 1 for a detailed description of each metric. Results of pairwise Tukey honest significant difference tests are provided for δ^{13}C and δ^{15}N signatures. Isotopic niche sizes, which were generated from 1000 bootstrap replicates, and years were assumed to be statistically different from each other if the 95% confidence intervals did not overlap.